

# ON TOPOLOGY OF THREE-DIMENSIONAL CONTINUA WITH SINGULAR POINTS\*

HAO LIANG<sup>†</sup>, YUNHAO QIU<sup>‡</sup>, YAN TAN<sup>‡</sup>, AND QINGHAI ZHANG<sup>‡§</sup>

**Abstract.** We propose to model the topology of three-dimensional (3D) continua by Yin sets, regular open semianalytic sets with bounded boundary. Our model differs from manifold-based models in that singular points of a 3D continuum, i.e., boundary points where the tangent plane is not uniquely defined, are treated not as anomalies but as a central subject of our theoretical investigation. We characterize the local and global topology of Yin sets. Then we give a unique boundary representation of Yin sets based on the notion of a glued surface, a quotient space of an orientable compact 2-manifold along a one-dimensional CW complex. Our results apply to 3D continua with arbitrarily complex topology and may be useful in a number of scientific and engineering applications such as solid modeling, computer-aided design, and numerical simulations of multiphase flows with topological changes.

**Key words.** Three-dimensional continua, singular points, multiphase flows, topological changes, computer-aided design, solid modeling.

**MSC codes.** 76T99, 68U07, 74A50

**1. Introduction.** The concept of a continuum is of fundamental significance in a vast number of scientific and engineering disciplines, such as continuum mechanics, solid modeling, and computer-aided design (CAD). Thus it is desirable to model continua both theoretically and algorithmically so as to describe their topology, approximate their geometry, and answer queries on derived quantities such as the normal vector, the interface curvature, and even the Betti numbers.

**1.1. Motivations from solid modeling and CAD.** There exist an array of continua models with varying mathematical rigor and application ranges. In the theoretical model of Requicha and Voelcker [19], continua in three dimensions (3D) are represented by r-sets, i.e., bounded regular closed semianalytic sets defined in Section 2; r-sets have been an essential mathematical tool for solid modeling since the dawning time of this field [20]. Unfortunately, as illustrated by [34, Fig. 5], the boundary representation (B-rep) of r-sets is not unique. For the uniqueness of the B-rep and the convenience of topological classification of 3D continua via their boundaries, it is desirable to have a new theoretical model where 3D continua and their boundaries have a one-to-one correspondence.

Algorithmically, the boundary of a 3D continuum  $\mathcal{Y}$  is often assumed to be a 2-manifold. Although this assumption leads to an efficient B-rep of  $\mathcal{Y}$ , it does not cover all legitimate cases of 3D continua. As shown in Figure 1, it is possible that a boundary point is a non-manifold point, cf. Definition 3.1, a particular type of singular points in Definition 3.2. These non-manifold points may cause, among other things, difficulties in the B-rep of 3D continua. In most CAD algorithms, the B-rep

\* Qinghai Zhang is the corresponding author. Author names are listed in the alphabetical ordering.

**Funding:** This work was supported by the National Natural Science Foundation of China (#12272346) and the Fundamental Research Funds for the Central Universities 226-2025-00254.

<sup>†</sup>School of Mathematics, Foshan University, Foshan, Guangdong, 528000, China. (lianghao1019@hotmail.com).

<sup>‡</sup>School of Mathematical Sciences, Zhejiang University, Hangzhou, Zhejiang, 310058, China. (qiyunhao@zju.edu.cn, yantanh@zju.edu.cn, qinghai@zju.edu.cn)

<sup>§</sup>Institute of Fundamental and Transdisciplinary Research, Zhejiang University, Hangzhou, Zhejiang, 310058, China.

surface of a 3D continuum is either assumed to be free of non-manifold/singular points or changed to a 2-manifold by removing such points [6].

Roughly speaking, the mesh data of current 3D continua models come either from digitizing real-world phenomena/objects or from synthesizing virtual data such as those created by human designers or computer programs such as a grid generator. Examples of digitized models include those in medical imaging [35], surface scanning [2], and 3D photography [24]; data in this category usually contain the so-called *defects* or *flaws* such as holes and self-intersections. Examples of synthetic models include sketch-based models [9], models with implicit mathematical formulations [28], and CAD systems [4]; data in this category are typically assembled from multiple parts and may contain other types of flaws such as overlaps, pairwise intersections, and self-intersections. Before these data can be used, their flaws have to be removed by a manual and tedious preprocessing known as *mesh repairing*, which has been under intense research; see [1] for a survey on how to select mesh repairers for given downstream applications. Things are made even more complicated by the fact that the precise definition of defects or flaws may vary according to the downstream applications. To sum up, singular points of 3D continua are theoretically treated as anomalies in CAD models and algorithmically handled on a case-by-case basis, leading to algorithmic complexity, code bloating, and high maintenance of the software.

From a physical viewpoint, some defects are *legitimate* in that it is possible for 3D objects or real phenomena to display them while others are *illegal* in that they cannot possibly exist in any physically meaningful 3D continua. For the examples shown in [1, Fig. 1], a singular vertex is legitimate while any hole, i.e., the missing of a triangle (a 2-simplex) in a closed surface (a 2-simplicial complex), is illegal. Indeed, as indicated by Figure 1(a), a singular vertex or a curve of such points may show up during merging or pinch-off. In contrast, any hole is illegal because it incurs an inconsistency in the B-rep of a 3D continuum. Therefore, for current algorithms in solid modeling and CAD, it might be useful to enumerate and classify all possible scenarios of singular points of 3D continua. Such a result is given in Theorem 6.3.

**1.2. Motivations from integrating CAD and CAE (Computer-Aided Engineering).** During the development of a new product, CAD systems help the developer with the geometric design of the prototype while CAE systems test its performance by computer simulations. For example, the shape and assembly of a water turbine are designed inside a CAD system such as AutoCAD™ while the performance of the turbine is tested inside a CAE system such as Fluent™. The feedback provided by the CAE system may lead to a change of the geometric design, which, in turn, leads to new CAE results; this process is usually repeated until both the shape and the performance of the updated prototype become acceptable.

Traditionally, CAD designers and CAE specialists are two disparate groups of people, whose communications are very limited and infrequent. Their distinct sets of skills and different viewpoints often lead to divergent opinions. Consequently, the iteration between CAD and CAE tends to be very slow and it often takes a long time to reach a consensus of the two parts.

With the fast advance of science, engineering, and industry, there has been a need to integrate CAD and CAE to speed up the pipeline of designing new products; see, e.g., [26, 7, 12] and references therein. In most of these efforts, CAD and CAE software are treated as black boxes and a middleware is developed to exchange data between them. One major issue of this approach is the almost unavoidable information loss between CAD and CAE, in which the two sets of data have, apart from the different

formats, more fundamental discrepancies. For example, the inconsistent definitions of tolerances make it difficult to rebuild the correct topology of CAD models for CAE. It is also a formidable task to bind different levels of geometric parts into integrity that is recognizable by CAE algorithms [3] [12, Fig. 1].

Based on the classification of *all* 3D continua in Theorem 6.3, we propose to separate the description of their topology from the approximation of their geometry. One obvious advantage of this B-rep approach is the ease of topology rebuilding and geometric integration during the process of data share and exchange: the topological structure is agnostic of geometric tolerances and different requirements of the geometric approximation do not affect the topology. When the shapes of a CAD model are specified via a set of rational parametric surfaces, one can use the outstanding algorithm by Jia, Chen, and Yao [10] to compute all singular points and combine Theorem 6.3 with the unique B-rep of 3D continua in Theorem 7.10 to integrate CAD and CAE with reduced information losses. Also, due to the almost disjoint surfaces in Definition 7.2, it is sometimes unnecessary for this integration to compute self-intersections [13] and overlap regions [29] of B-rep surfaces.

**1.3. Motivations from interface tracking (IT) in simulating multiphase flows.** In computational physics, recent advances of numerically solving partial differential equations on moving domains call for high-fidelity simulations that integrate CAD models of complex topology/geometry with CAE algorithms/analysis. One such field is the study of multiphase flows.

In drastic comparison to solid modeling, a rigorous model of the topology and geometry of 3D continua appears to be absent in continuum mechanics; this is particularly true in computational fluid dynamics and multiphase flows. In a sharp-interface model of multiphase flows, each phase is represented by a moving continuum, which evolves according to the governing equations and the interface/boundary conditions. Each phase may undergo large geometric deformations and even topological changes. The accurate IT of these phases is crucial in numerically simulating multiphase flows, because the IT error not only leads to a lower bound on estimation errors of the normal vector and interface curvature [31], but also adversely affects the accuracy of simulating the flow field.

Currently, popular IT methods include the volume-of-fluid (VOF) method [8], the level-set method [16], and the front tracking method [27]. In VOF methods, the region occupied by a fluid phase  $M$  is modeled by the point set  $\mathcal{M}(t) := \{\mathbf{x} : \chi(\mathbf{x}, t) = 1\}$  where the *color function*  $\chi(\mathbf{x}, t)$  is 1 if there is  $M$  at  $(\mathbf{x}, t)$  and 0 otherwise. At each time  $t$ ,  $\mathcal{M}(t)$  is implicitly represented by volume fractions of  $\chi$  in all control volumes. Within a given time interval,  $\mathcal{M}(t)$  is evolved by numerically solving the governing equation of  $\chi$ , be it the scalar conservation law or the advection equation. In level-set methods, an interface is implicitly represented as the zero isocontour of a signed distance function, and is tracked by numerically solving the scalar conservation law or the advection equation. In the front tracking method [27], the boundary of a phase is explicitly represented by a set of connected Lagrangian markers and the IT of this phase is reduced to tracking these markers via numerically solving ordinary differential equations. In all of the aforementioned IT methods, *topological and geometric problems in IT are avoided as they are converted to numerically solving differential equations.*

Our approach to IT is fundamentally different: *we tackle topological and geometric problems in IT with tools in topology and geometry.* This principle of *fluid modeling* has been directing our work in two dimensions (2D): we have established a model of 2D

continua called Yin sets [34], completely classified all 2D Yin sets, designed a unique B-rep of 2D continua, equipped the Yin sets with a natural Boolean algebra, proposed an analytic framework called MARS (mapping and adjusting regular semianalytic sets) for analyzing explicit IT methods [33], and developed several MARS methods [32, 25] for high-order IT in 2D. By performing standard benchmark tests for both two-phase IT [32] and three-or-more-phases IT [25], we have shown that the MARS methods are superior over current IT methods in terms of accuracy, efficiency, and preserving topological structures and geometric features. Given the explicit modeling of 2D fluids, the supremacy of MARS methods is not surprising.

A major motivation of this work is the generalization of fluid modeling from 2D to 3D. As a fundamental difference of IT from CAD, the singular points that characterize topological changes of a continuum should never be removed. Instead, these singular points should be in the spotlight of both theory and algorithms so that homeomorphic deformations and topological changes of a 3D continuum can be handled accurately and efficiently for arbitrarily complex topology.

**1.4. Contributions of this work.** The above discussions sum up to questions as follows.

- (Q-1) Can we design, from a minimum set of natural physical constraints, a 3D continua model that neither includes nonphysical singular points nor excludes the legitimate ones?
- (Q-2) Can we rigorously characterize the local and global topology of 3D continua with singular points?
- (Q-3) Based on different types of intersections in Definition 4.2 and the answer to (Q-2), can we uniquely represent each 3D continuum by a set of surfaces that are free of overlaps, self-intersections, and proper pairwise intersections?

In this work, we give positive answers to all the above questions by generalizing Yin sets from 2D to 3D; this is also our first step in 3D fluid modeling.

In Section 2, we briefly review the Yin space proposed in [34]; it is fortuitous that the Yin space originally designed for 2D continua worked out in 3D without any modifications. The 3D Yin space is also our answer to (Q-1). In Section 3, we define several types of singular points to include all characteristic boundary points of a 3D Yin set. In Section 4, we define a surface as an orientable compact 2-manifold and introduce the important notions of proper and improper intersections of surfaces. In Section 5, we examine the local topology of 3D continua by focusing on the good neighborhood of singular points. The key concept of good pairing in Subsection 5.4 leads to Theorem 6.3 on the global topology, which answers (Q-2). Different from the 2D case, it is not obvious how to deduce a unique B-rep of 3D continua from the main theorem on the global topology. In Section 7, we define the new concept of glued surfaces, employ it as the basic building block in decomposing the boundary of a 3D continuum, and show in Theorem 7.10 that any connected 3D Yin set can be uniquely represented by a set of oriented glued surfaces. Apart from answering (Q-3), this unique 3D B-rep has the same form as that of the 2D case, with glued surfaces replacing the Jordan curves in [34, eq. (3.6)]. Finally in Section 8, we conclude this paper with several future research prospects.

**2. The Yin space.** In a topological space  $\mathcal{X}$ , the *complement* of a subset  $\mathcal{P} \subseteq \mathcal{X}$ , written  $\mathcal{P}'$ , is the set  $\mathcal{X} \setminus \mathcal{P}$ . The *closure* of a set  $\mathcal{P} \subseteq \mathcal{X}$ , written  $\overline{\mathcal{P}}$ , is the intersection of all closed supersets of  $\mathcal{P}$ . The *interior* of  $\mathcal{P}$ , written  $\mathcal{P}^\circ$ , is the union of all open subsets of  $\mathcal{P}$ . The *exterior* of  $\mathcal{P}$ , written  $\mathcal{P}^\perp := \mathcal{P}'^\circ := (\mathcal{P}')^\circ$ , is the interior of its complement. By the identity  $\overline{\mathcal{P}} = \mathcal{P}'^\circ$  [5, p. 58], we have  $\mathcal{P}^\perp = \overline{\mathcal{P}'}$ . A point  $\mathbf{x} \in \mathcal{X}$  is

a *boundary point* of  $\mathcal{P}$  if  $\mathbf{x} \notin \mathcal{P}^\circ$  and  $\mathbf{x} \notin \mathcal{P}^\perp$ . The *boundary* of  $\mathcal{P}$ , written  $\partial\mathcal{P}$ , is the set of all boundary points of  $\mathcal{P}$ . It can be shown that  $\mathcal{P}^\circ = \mathcal{P} \setminus \partial\mathcal{P}$  and  $\overline{\mathcal{P}} = \mathcal{P} \cup \partial\mathcal{P}$ . A set  $\mathcal{P} \subseteq \mathcal{X}$  is *regular open* if it coincides with the interior of its own closure, i.e. if  $\mathcal{P} = \overline{\mathcal{P}^\circ}$ , and is *regular closed* if it coincides with the closure of its own interior, i.e. if  $\mathcal{P} = \overline{\mathcal{P}^\circ}$ . The duality of the interior and closure operators implies  $\mathcal{P}^\circ = \overline{\mathcal{P}'}$ , hence  $\mathcal{P}$  is a regular open set if and only if  $\mathcal{P} = \mathcal{P}^{\perp\perp} := (\mathcal{P}^\perp)^\perp$ . For any subset  $Q \subseteq \mathcal{X}$ , it can be shown that  $Q^{\perp\perp}$  is a regular open set and  $\overline{Q^\circ}$  is a regular closed set.

Regular sets, open or closed, capture the salient feature that continua are free of lower-dimensional elements such as isolated points and curves in  $\mathbb{R}^2$  and dangling faces in  $\mathbb{R}^3$ . However, regular sets are not perfect for representing physically meaningful regions yet: some of them cannot be described by a finite number of symbol structures. For example, some sets have nowhere differentiable boundaries, which, in their parametric forms, are usually infinite series of continuous functions [22]. Another pathological case is more subtle: intersecting two regular sets may yield an infinite number of disjoint regular sets. Consider

$$(2.1) \quad \begin{cases} \mathcal{A}_p := \{(x, y) \in \mathbb{R}^2 : -2 < y < \sin \frac{1}{x}, 0 < x < 1\}, \\ \mathcal{A}_s := \{(x, y) \in \mathbb{R}^2 : 0 < y < 1, -1 < x < 1\}. \end{cases}$$

Although both  $\mathcal{A}_p$  and  $\mathcal{A}_s$  are described by two inequalities, their intersection is a disjoint union of an infinite number of regular sets; see [18, Fig. 4-1, Fig. 4-2]. This poses a fundamental problem that results of Boolean operations of two regular sets may not be well represented on a computer by a finite number of entities.

Therefore, we need to find a proper subspace of regular sets, each element of which is finitely describable. This search eventually arrives at semianalytic sets.

**DEFINITION 2.1** (Semianalytic sets). *A set  $\mathcal{S} \subseteq \mathbb{R}^D$  is semianalytic if there exist a finite number of analytic functions  $g_i : \mathbb{R}^D \rightarrow \mathbb{R}$  such that  $\mathcal{S}$  is in the universe of a finite Boolean algebra formed from the sets*

$$(2.2) \quad \mathcal{X}_i = \{\mathbf{x} \in \mathbb{R}^D : g_i(\mathbf{x}) \geq 0\}.$$

The  $g_i$ 's are called the *generating functions* of  $\mathcal{S}$ . In particular, a semianalytic set is semialgebraic if all of its generating functions are polynomials.

Recall that a function is *analytic* if and only if its Taylor series at  $\mathbf{x}_0$  converges to the function in some neighborhood for every  $\mathbf{x}_0$  in its domain. In the example of (2.1),  $\mathcal{A}_s$  is semianalytic while  $\mathcal{A}_p$  is not, because the Taylor series of  $g_2(x, y) := \sin \frac{1}{x} - y$  at the origin does not converge. Roughly speaking, the boundary curves of regular semianalytic sets are piecewise smooth.

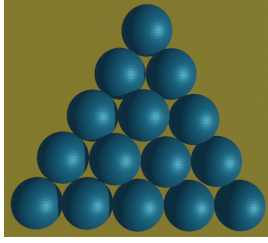
As mentioned in the opening paragraph of Subsection 1.1, the B-rep of regular closed sets is not unique. In addition, the analysis of explicit IT methods via the theory of donating regions [30] also requires that the regular sets be open. Therefore, only regular open semianalytic sets are employed in this work.

**DEFINITION 2.2.** *A Yin set<sup>1</sup>  $\mathcal{Y} \subseteq \mathbb{R}^D$  ( $D = 2, 3$ ) is a regular open semianalytic set whose boundary is bounded. The class of all such Yin sets form the Yin space  $\mathbb{Y}$ .*

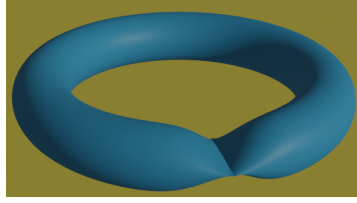
In this work we focus on the 3D case; see Figure 1 for examples of 3D Yin sets.

---

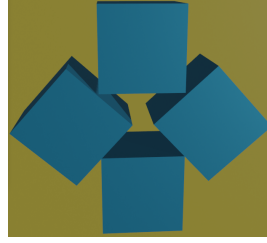
<sup>1</sup>Yin sets are named after Qinghai Zhang's mentor, Madam Ping Yin. As a coincidence, the most important dichotomy in Taoism consists of Yin and Yang, where Yang represents the active, the straight, the ascending, and so on, while Yin represents the passive, the circular, the descending, and so on. From this viewpoint, straight lines and Jordan curves can be considered as Yang 1-manifolds and Yin 1-manifolds, respectively.



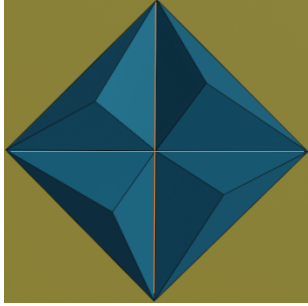
(a) each singular point is an isolated non-manifold point with unique tangent plane



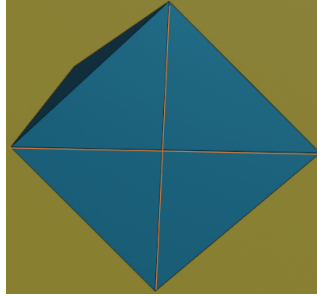
(b) all singular points are non-isolated non-manifold points in one connected component



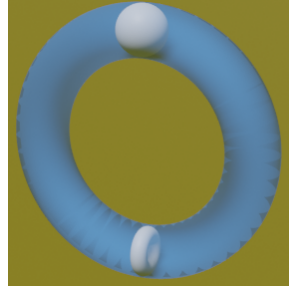
(c) all non-manifold points are non-isolated and in multiple connected components



(d) all non-isolated non-manifold points are in a single connected component consisting of two intersecting curves (top view)



(e) the bottom view of the Yin set in (d); the four endpoints and the intersection of the two yellow lines are vertex non-manifold points



(f) all singular points are non-manifold, non-isolated, and in two connected components, each of which is a Jordan curve

FIG. 1. Examples of 3D Yin sets and singular points on their boundaries. The Yin set in (d) consists of four tetrahedrons whose bottom edges touch upon each other along the two yellow lines. Each connected component of a Yin set in (a-e) is homeomorphic to the unit open ball while the Yin set in (f) is not: it is obtained by removing a sphere and a small torus from the big solid torus. The Yin sets in (a,b,f) only have non-manifold singular points while those in (c-e) also contain kinks.

**3. Singular points of a Yin set.** In this section, we capture all characteristic points of a Yin set in the definition of singular points and give several different dichotomies of them to facilitate the analysis and the unique B-rep in later sections.

**DEFINITION 3.1 (Manifold/non-manifold points).** A boundary point  $p$  of a Yin set  $\mathcal{Y} \subset \mathbb{R}^3$  is called a manifold point of  $\partial\mathcal{Y}$  if there exists a sufficiently small open ball  $\mathcal{N}(p) \subset \mathbb{R}^3$  centered at  $p$  such that  $\mathcal{N}(p) \cap \partial\mathcal{Y}$  is homeomorphic to the unit open disk in  $\mathbb{R}^2$ ; otherwise  $p$  is a non-manifold point of  $\partial\mathcal{Y}$ .

**DEFINITION 3.2 (Singular/non-singular points).** A boundary point  $p$  of a Yin set  $\mathcal{Y} \subset \mathbb{R}^3$  is singular if  $p$  is a non-manifold point or the tangent plane of  $\partial\mathcal{Y}$  at  $p$  is not uniquely defined; otherwise  $p$  is non-singular.

By Definitions 3.1 and 3.2, a non-manifold point is always a singular point; conversely, a singular point is either a non-manifold point or a *kink*, i.e., a manifold point of  $\partial\mathcal{Y}$  with  $\mathcal{C}^1$  discontinuity.

**DEFINITION 3.3 (Isolated/non-isolated non-manifold points).** A non-manifold point  $p \in \partial\mathcal{Y}$  is isolated if  $p$  is the only non-manifold point in  $\mathcal{N}(p) \cap \partial\mathcal{Y}$  for some sufficiently small open ball  $\mathcal{N}(p) \subset \mathbb{R}^3$  centered at  $p$ ; otherwise  $p$  is non-isolated.

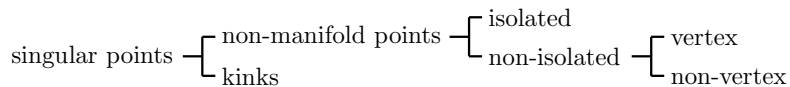


FIG. 2. The relations of various singular points.

DEFINITION 3.4 (Vertex/non-vertex non-manifold points). *A non-isolated non-manifold point  $p$  of a Yin set  $\mathcal{Y}$  is said to be non-vertex non-manifold if there exists a sufficiently small  $\mathcal{N}(p) \subset \mathbb{R}^3$  such that the set of all non-isolated non-manifold points in  $\mathcal{N}(p) \cap \partial\mathcal{Y}$  is homeomorphic to  $(0, 1)$ ; otherwise  $p$  is vertex non-manifold.*

In a sufficiently small neighborhood of a vertex non-manifold point  $p$ , the set of non-isolated non-manifold points is homeomorphic either to  $[0, 1)$  or to a *star*, i.e., the union of three or more curves which intersect at their common endpoint  $p$  and are otherwise pairwise disjoint.

By Definitions 3.3 and 3.4, each non-manifold point of a Yin set is either isolated or non-isolated; each non-isolated non-manifold point is either vertex non-manifold or non-vertex non-manifold. The three sets of isolated, vertex, or non-vertex non-manifold points are pairwise disjoint; see Figure 2 for relations of these singular points and Figure 1 for some examples.

In a similar manner, we can also define isolated, vertex, and non-vertex kinks, but their topology is usually simpler than (or at most similar with) that of non-manifold points. Therefore in this work we do not study them except in Lemma 5.10.

**4. A surface is a piecewise-smooth orientable compact 2-manifold.** An *m-manifold* is a second countable Hausdorff space that is locally homeomorphic to  $\mathbb{R}^m$ . For example, a 1-manifold could be a Jordan curve, a line, or a Jordan curve minus one point; a 2-manifold could be a simple closed surface or an *open surface patch*, i.e., the homeomorphic image of  $(0, 1)^2$  under a continuous map  $(0, 1)^2 \mapsto \mathbb{R}^3$ . An *m-manifold with boundary* is the union of an  $m$ -manifold  $\mathcal{S}$  and an  $(m-1)$ -manifold that is the boundary of  $\mathcal{S}$ . Consider the *n-disk* and the *n-sphere*,

$$(4.1) \quad \mathbb{D}^n := \{\mathbf{x} \in \mathbb{R}^n : \|\mathbf{x}\| \leq 1\}; \quad \mathbb{S}^n := \{\mathbf{x} \in \mathbb{R}^{n+1} : \|\mathbf{x}\| = 1\}.$$

$\mathbb{D}^2$  is a 2-manifold with boundary and  $\mathbb{S}^1$  is the 1-manifold boundary of  $\mathbb{D}^2$ .

For a smooth compact 2-manifold  $\mathcal{S}$ , the tangent space  $T_p$  of  $p \in \mathcal{S}$  is a 2D real vector space. Two bases  $(\mathbf{v}_1, \mathbf{v}_2)$  and  $(\mathbf{u}_1, \mathbf{u}_2)$  of  $T_p$  define the same orientation if the sign of the determinant of the change-of-basis matrix from  $(\mathbf{v}_1, \mathbf{v}_2)$  to  $(\mathbf{u}_1, \mathbf{u}_2)$  is  $+$ ; otherwise they define different orientations. This binary relation of “defining the same orientation” is an equivalence relation on all bases of  $T_p$  and each of the two equivalence classes is called an *orientation of the tangent space  $T_p$* . The *orientation of a point  $p \in \mathcal{S}$*  is identified with that of  $T_p$ .

A smooth compact 2-manifold  $\mathcal{S}$  is *orientable* if each point in  $\mathcal{S}$  can be assigned an orientation such that any two points sufficiently close have the same orientation. A piecewise-smooth compact 2-manifold  $\mathcal{S}$  is *orientable* if it can be approximated arbitrarily well by a smooth orientable compact 2-manifold.

DEFINITION 4.1 (Surface). *A surface is a piecewise-smooth orientable compact 2-manifold and a surface with boundary is a piecewise-smooth orientable compact 2-manifold with boundary.*

The following concepts of proper and improper intersections are crucial in the unique B-rep of Yin sets, cf. Definition 7.2; also see Figure 3 for an illustration.

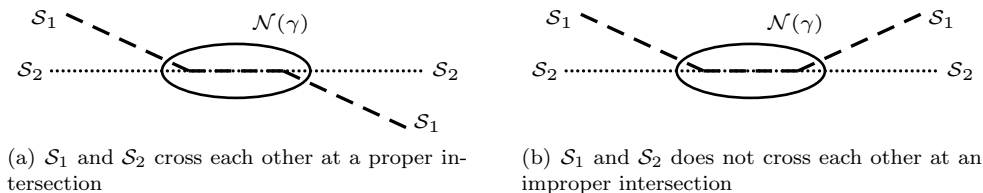


FIG. 3. Examples of proper and improper intersections in Definition 4.2.

DEFINITION 4.2 (Intersections of surfaces and/or surfaces with boundary). *Let  $\mathcal{S}_1$  and  $\mathcal{S}_2$  be two surfaces or surfaces with boundary; they are disjoint if  $\mathcal{S}_1 \cap \mathcal{S}_2 = \emptyset$ . Otherwise a maximally connected component  $\gamma$  of  $\mathcal{S}_1 \cap \mathcal{S}_2$  is called an improper intersection of  $\mathcal{S}_1$  and  $\mathcal{S}_2$  if  $(\mathcal{S}_2 \cap \mathcal{N}(\gamma)) \setminus \gamma$  is contained in a single component of  $\mathcal{N}(\gamma) \setminus \mathcal{S}_1$  in a sufficiently small open neighborhood  $\mathcal{N}(\gamma) \subset \mathbb{R}^3$ ; otherwise  $\gamma$  is a proper intersection.*

The following celebrated theorem is one of the early triumphs of algebraic topology; see [15, Chap. 1] for a proof.

THEOREM 4.3 (Classification of surfaces). *Every surface is homeomorphic to a 2-sphere, a torus, or a connected sum of tori.*

A simple closed curve is homeomorphic to  $\mathbb{S}^1$  and its complement in  $\mathbb{R}^2$  consists of two connected components: one bounded and the other unbounded; this is the classical Jordan curve theorem [11]. For  $n \geq 2$ , the Jordan–Brouwer separation theorem states that the complement of  $\mathbb{S}^{n-1}$  in  $\mathbb{R}^n$  also consists of two connected components: one bounded and the other unbounded; see [21, Theorem 6.35]. In the particular case of  $n = 3$ , the conclusion of the Jordan–Brouwer separation theorem also holds for a surface [14, 23]. This dichotomy of surface complement into bounded and unbounded components is of fundamental importance in defining the key concept of glued surfaces in Definition 7.1.

DEFINITION 4.4 (Orientations of a surface). *For a surface  $\mathcal{S}$  whose orientation is indicated by a basis  $(\mathbf{v}_1, \mathbf{v}_2)$  of the tangent space  $T_p\mathcal{S}$ , we regard  $\mathbf{v}_1$  and  $\mathbf{v}_2$  as vectors in  $\mathbb{R}^3$  by the embedding of  $T_p\mathcal{S}$  in  $T_p\mathbb{R}^3$  and define the induced normal vector  $\mathbf{n}$  at  $p \in \mathcal{S}$  as the vector induced from the right-hand rule to form a basis  $(\mathbf{v}_1, \mathbf{v}_2, \mathbf{n})$  of  $\mathbb{R}^3$ . The surface  $\mathcal{S}$  is positively oriented if  $\mathbf{n}$  always points from its bounded complement to its unbounded complement; otherwise it is negatively oriented.*

DEFINITION 4.5 (Internal complement of a surface). *The internal complement of a surface  $\mathcal{S}$ , written  $\text{int}(\mathcal{S})$ , is its bounded complement if  $\mathcal{S}$  is positively oriented and its unbounded complement if  $\mathcal{S}$  is negatively oriented.*

Definitions 4.4 and 4.5 pave the way to the unique B-rep in Theorem 7.10.

**5. Local topology.** For an interior point or a manifold point of a Yin set, its local neighborhood has the trivial topology of a ball or a half ball, respectively. So we are mostly interested in the local topology of non-manifold points.

**5.1. The good neighborhood of a boundary point.** We start with

DEFINITION 5.1 (Generalized disk). *For a Yin set  $\mathcal{Y}$ , a generalized disk  $\mathcal{D}$  at a boundary point  $p \in \partial\mathcal{Y}$  within an open ball  $\mathcal{N}(p) \subset \mathbb{R}^3$  is the homeomorphic image of  $\mathbb{D}^2$  in (4.1) under a continuous map  $f : \mathbb{D}^2 \rightarrow \partial\mathcal{Y} \cap \mathcal{N}(p)$ , such that  $p = f(\mathbf{0})$  and*

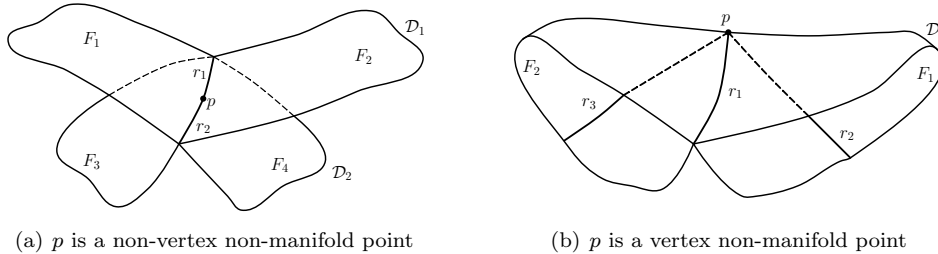


FIG. 4. *Examples of generalized disks, generalized radii, and generalized sectors. In (a), each of the four sectors is on both  $r_1$  and  $r_2$ ; each of the two disks is the union of two sectors:  $\mathcal{D}_1 = F_1 \cup F_2$  and  $\mathcal{D}_2 = F_3 \cup F_4$ . In (b),  $\partial\mathcal{Y} \cap \overline{\mathcal{N}(p)}$  is a folded disk in Definition 5.11 with  $k = 2$  and  $t = 1$ . Originally, both of the two sectors  $F_1$  and  $F_2$  with  $\mathcal{D} = F_1 \cup F_2$  are on the radius  $r_1$ ; the artificial radii  $r_2$  and  $r_3$  are added according to Convention 5.4 so that each of  $F_1$  and  $F_2$  are on two radii.*

$f(\mathbb{S}^1) \subset \partial\mathcal{N}(p)$ , where  $\mathbb{S}^1$  is the boundary of  $\mathbb{D}^2$  and  $f(\mathbb{S}^1)$  is called the boundary of the generalized disk, written  $\partial\mathcal{D}$ .

In Figure 1(a), each isolated singular point is the intersection of two generalized disks. By Definitions 3.3 and 5.1, a boundary point  $p \in \partial\mathcal{Y}$  is non-singular if and only if  $p$  is not a kink and the number of generalized disks at  $p$  is 1.

**DEFINITION 5.2 (Generalized radius).** *For a Yin set  $\mathcal{Y}$ , a generalized radius of a boundary point  $p \in \partial\mathcal{Y}$  within an open ball  $\mathcal{N}(p) \subset \mathbb{R}^3$  centered at  $p$  is a simple curve  $\gamma \subset \partial\mathcal{Y}$  from  $p$  to some point in  $\partial\mathcal{Y} \cap \partial\mathcal{N}(p)$ .*

The main purpose of a generalized radius is to represent (part of) a connected component of non-isolated non-manifold points. In Figure 1(b), all non-manifold points are non-isolated and they constitute a single simple curve  $\gamma : [0, 1] \rightarrow \partial\mathcal{Y}$ , of which the endpoints are vertex non-manifold and all other points are non-vertex non-manifold. For each non-vertex non-manifold point  $p$ , the set of all non-isolated non-manifold points in a sufficiently small neighborhood  $\mathcal{N}(p)$  is the union of two generalized radii which intersect only at  $p$ ; see Figure 4(a). In contrast, for a vertex non-manifold point  $p_v$  of  $\gamma$ , a single generalized radius  $r_v$  at  $p_v$  might contain all non-isolated non-manifold points in  $\mathcal{N}(p_v) \cap \partial\mathcal{Y}$ ; see Figure 4(b).

In Figure 1(c), non-manifold points constitute four pairwise distinct simple curves. In the neighborhood of a vertex non-manifold point  $q_\gamma$  of each curve  $\gamma$ , the set of all non-isolated non-manifold points is a single generalized radius  $r_q$  at  $q_\gamma$ .

**DEFINITION 5.3 (Generalized sector).** *For a boundary point  $p \in \partial\mathcal{Y}$  of a Yin set  $\mathcal{Y}$ , two distinct generalized radii  $r_1$  and  $r_2$  of  $p$  in a generalized disk  $\mathcal{D}$  centered at  $p$  cut  $\mathcal{D}$  into two connected components whose boundaries relative to  $\mathcal{D}$  are both  $r_1 \cup r_2$ . The closure of each of the two connected components is called a generalized sector with  $r_1$  and  $r_2$  as the generalized radii of this sector. If  $r$  is a generalized radius of a sector  $F$ , then  $F$  is called a generalized sector on  $r$ .*

In Figure 1(d,e), the single connected component of non-manifold points can be considered as the union of two line segments intersecting only at a vertex non-manifold point, whose local neighborhood contains four generalized radii and eight generalized sectors, with four generalized sectors on each generalized radius.

In the aforementioned example of Figure 1(c), there exists a sector  $F$  in  $\mathcal{N}(q_\gamma)$  of which both generalized radii are  $r_q$ . Similarly, in Figure 1(b), each of the two sectors in  $\mathcal{N}(p_v)$  is on  $r_v$  and only on  $r_v$ . These special cases motivate

CONVENTION 5.4. *Whenever a sector  $F$  is on a single radius  $r$ , we pick another radius  $r'$  in  $F$  intersecting  $r$  only at  $p$ , so that  $r$  and  $r'$  divide  $F$  into two sectors.*

The “artificial” generalized radius  $r'$  is different from  $r$  in that  $r' \setminus \{p\}$  consists of only manifold points of  $\mathcal{Y}$ . Convention 5.4 will be convenient in later analysis since, although the number of sectors may vary from one good neighborhood to another, the number of sectors on each radius  $r$  is always even.

All the aforementioned examples in Figure 1 are special cases of

LEMMA 5.5 (Local topology of a boundary point). *For a boundary point  $p$  of a 3D Yin set  $\mathcal{Y}$ , any sufficiently small open neighborhood  $\mathcal{N}(p) \subset \mathbb{R}^3$  satisfies*

- (a)  $\partial\mathcal{Y} \cap \overline{\mathcal{N}(p)}$  is the union of finitely many generalized disks;
- (b) Pairwise intersection of the generalized disks in (a) is either  $p$  itself or the union of finitely many generalized radii pairwise intersecting only at  $p$ ;
- (c)  $\mathcal{N}(p) \setminus \partial\mathcal{Y}$  consists of disjoint regular open sets; two such sets sharing a common sector as part of their boundary are subsets of  $\mathcal{Y}$  and  $\mathcal{Y}^\perp$ , respectively.

*Proof.* By Definition 2.1 and  $\mathcal{Y}$  being semianalytic,  $\partial\mathcal{Y} \cap \mathcal{N}(p)$  is defined by a finite number of analytic functions  $g_i : \mathbb{R}^3 \rightarrow \mathbb{R}$ , each of which can be replaced by its Taylor series expanded at  $p$ . Thus each  $g_i$  can be approximated arbitrarily well, within a sufficiently small open neighborhood  $\mathcal{N}(p)$ , by a linear function of the form  $\tilde{g}_i(x, y, z) = a_0 + a_1x + a_2y + a_3z$ . Hence the points satisfying  $g_i(x, y, z) = 0$  can be regarded as the graph of some linear height function  $\chi = H_i(\xi, \eta)$ . Therefore,  $\partial\mathcal{Y} \cap \overline{\mathcal{N}(p)}$  can only contain the homeomorphic images of  $\mathbb{D}^2$ , which, by Definition 5.1, are generalized disks. Therefore (a) holds.

The intersection of any two distinct generalized disks in (a) contains no 2D components; otherwise it would contradict Definition 2.2 that any Yin set is regular open. By Definition 5.1, each generalized disk is a surface with boundary and is thus triangularizable. Consequently,  $\mathcal{Y} \cap \mathcal{N}(p)$  can be approximated arbitrarily well, within a sufficiently small neighborhood  $\mathcal{N}(p)$ , by a semianalytic set whose generating functions are multivariate linear polynomials corresponding to triangles in the triangular mesh. The intersection of two such triangular meshes is either  $p$  itself or a finite number of curves intersecting only at  $p$ . Therefore (b) holds.

By (a) and (b), we get a finite number of disjoint regular open sets after deleting from  $\mathcal{N}(p)$  a finite number of surfaces. For two such regular open sets sharing a common sector, both cannot be contained in  $\mathcal{Y}$  because this would contradict  $\mathcal{Y}$  being regular open. Similarly, both cannot be contained in  $\mathcal{Y}^\perp$  either. Hence (c) holds.  $\square$

DEFINITION 5.6 (Good neighborhood). *A good neighborhood of a boundary point  $p \in \partial\mathcal{Y}$  is a sufficiently small open set  $\mathcal{N}(p) \supset p$  satisfying (i)  $\mathcal{N}(p)$  is homeomorphic to the interior of  $\mathbb{D}^3$  and (ii) the conclusions of Lemma 5.5 hold in  $\mathcal{N}(p)$ .*

By Lemma 5.5, the type of a boundary point  $p \in \partial\mathcal{Y}$  and the topology of  $\partial\mathcal{Y} \cap \mathcal{N}(p)$  are independent of the choice of the good neighborhood  $\mathcal{N}(p)$ .

NOTATION 5.7. *Hereafter a good neighborhood of a singular point  $p$  will be denoted by  $\mathcal{N}(p)$ . A disk refers to a generalized disk in  $\partial\mathcal{Y} \cap \overline{\mathcal{N}(p)}$  given by Lemma 5.5(a), a radius refers to a generalized radius along which multiple disks in  $\overline{\mathcal{N}(p)}$  intersect, cf. Definition 5.2, and a sector refers to a generalized sector on a radius as in Definition 5.3. The collection of all radii in  $\overline{\mathcal{N}(p)}$  is denoted by  $\mathcal{R}(p)$ .*

**5.2. The global topology of singular points.** The disjoint union  $\mathcal{U}_\mathcal{X}$  of a family  $\{\mathcal{X}_\alpha\}_{\alpha \in J}$  of topological spaces is given by

$$(5.1) \quad \mathcal{U}_\mathcal{X} := \sqcup_{\alpha \in J} \mathcal{X}_\alpha := \cup_{\alpha \in J} \mathcal{U}_\alpha \quad \text{where } \mathcal{U}_\alpha := \mathcal{X}_\alpha \times \{\alpha\}.$$

If we topologize  $\mathcal{U}_{\mathcal{X}}$  by declaring  $U$  to be open in  $\mathcal{U}_{\mathcal{X}}$  if and only if  $U \cap \mathcal{U}_{\alpha}$  is open in  $\mathcal{U}_{\alpha}$  for each  $\alpha$ , then  $\mathcal{U}_{\mathcal{X}}$  is said to be the *topological sum* of the spaces  $\mathcal{U}_{\alpha}$  or  $\mathcal{X}_{\alpha}$ .

DEFINITION 5.8 (Attaching space/map). *For two topological spaces  $\mathcal{X}_1, \mathcal{X}_2$ , and a continuous function  $f : B \rightarrow A$  with  $A \subset \mathcal{X}_1$  and  $B \subset \mathcal{X}_2$ , the attaching space of  $\mathcal{X}_1$  and  $\mathcal{X}_2$ , written  $\mathcal{X}_1 \sqcup_f \mathcal{X}_2$ , is the quotient space of the topological sum  $\mathcal{X}_1 \sqcup \mathcal{X}_2$  obtained by identifying each  $a \in A$  with every  $b \in f^{-1}(a)$ . Then the continuous function  $f$  is called the attaching map of  $\mathcal{X}_1 \sqcup_f \mathcal{X}_2$ .*

In this work the attaching map is assumed to be well behaved so that the attaching space always has the quotient topology. For example, let  $\mathcal{X}_2 = \mathbb{D}^2$ ,  $B = \partial\mathcal{X}_2$ , and  $\mathcal{X}_1 = A$  be the space of one point. For the attaching map  $f : B \rightarrow A$  that collapses  $B$  to the single point in  $A$ , the attaching space  $\mathcal{X}_1 \sqcup_f \mathcal{X}_2$  is homeomorphic to  $\mathbb{S}^2$ .

DEFINITION 5.9 (1D CW complex). *A one-dimensional (1D) CW complex  $K_1$  is an attaching space constructed from 0-cells (points)  $p_1, p_2, \dots, p_{k_0}$ , 1-cells (curve segments homeomorphic to  $\mathbb{D}^1$ )  $\gamma_1, \gamma_2, \dots, \gamma_{k_1}$  and an attaching map  $f$  as follows.*

- (a) *The 0-skeleton of  $K_1$  is the disjoint union of its 0-cells, written  $K^{(0)} := \sqcup_{i=1}^{k_0} p_i$ ;*
- (b) *Build the 1-skeleton as an attaching space  $K^{(1)} := C^1 \sqcup_f K^{(0)}$ , where the attaching map has the signature  $f : \partial C^1 \rightarrow K^{(0)}$  and  $C^1 := \sqcup_{j=1}^{k_1} \gamma_j$ ;*
- (c) *The 1-skeleton is taken to be the cell complex, i.e.,  $K_1 := K^{(1)}$ .*

A 1D CW complex is always homeomorphic to a graph  $G = (V, E, \phi_G)$ , where the incidence function  $\phi_G : E \rightarrow V \times V$  can be deduced directly from the attaching map. When the degree of each vertex in  $V$  is either 2 or 1, a 1D CW complex is either a 1-manifold or a 1-manifold with boundary; otherwise it is not a 1-manifold. For a Yin set shown in Figure 1, a connected component of its singular points may be one isolated singular point (subplot (a)), a curve segment (subplot (b)), a 1-manifold (subplot (f)), or some 1D subset that is neither a 1-manifold nor a 1-manifold with boundary (subplots (c,d,e)). All these examples are special cases of

LEMMA 5.10. *Any Yin set  $\mathcal{Y} \subset \mathbb{R}^3$  satisfies*

- (a)  *$\partial\mathcal{Y}$  contains finitely many isolated singular points;*
- (b) *the non-manifold points of  $\partial\mathcal{Y}$  form a 1D CW complex, so do the manifold singular points of  $\partial\mathcal{Y}$ .*

*Proof.* By Definition 2.2,  $\partial\mathcal{Y}$  is compact. Suppose  $\partial\mathcal{Y}$  contains infinitely many isolated singular points. Then there must exist a point  $y \in \partial\mathcal{Y}$  such that any neighborhood  $\partial\mathcal{Y} \cap \mathcal{N}(y)$  contains infinitely many isolated singular points. By Definition 2.1, none of the neighborhood of  $y$  is a good neighborhood, and this contradicts Lemma 5.5. Therefore (a) holds. As for (b), we only consider the case of non-manifold points since the proof for manifold singular points is similar.

Let  $l$  be a connected component of the set of all non-manifold singular points. For any  $p \in l$ ,  $l \cap \mathcal{N}(p)$  is homeomorphic to  $\bigcup_{r \in \mathcal{R}(p)} r$ , where all radii intersect only at  $p$ . So  $l$  is locally homeomorphic to a star in a graph. Therefore  $l$  is homeomorphic to a graph and hence can be given the structure of a 1D CW complex.

To show that the set of non-manifold points is closed in  $\partial\mathcal{Y}$ , we show that any convergent sequence of non-manifold points converges to a non-manifold point. Suppose the point  $q$  to which the sequence converges is not a non-manifold point. Then  $q$  is a manifold point and Definition 3.1 implies the existence of a good neighborhood of  $q$  that contains none of the non-manifold points, which contradicts the convergence of the sequence. Therefore the set of non-manifold points must be compact.  $\square$

The homeomorphism between the 1D CW complex in Lemma 5.10(b) and a

graph explains the names “vertex non-manifold points” and “non-vertex non-manifold points” in Definition 3.4.

**5.3. Folded disks.** By setting both  $\mathcal{X}_1$  and  $\mathcal{X}_2$  in Definition 5.8 to a generalized disk and requiring that the attaching map preserves all radii, we get

DEFINITION 5.11. *A folded disk is the attaching space of a generalized disk via an attaching map  $f : r_1 \cup \dots \cup r_k \rightarrow l_1 \cup \dots \cup l_t$  such that (i)  $r_1, \dots, r_k$  and  $l_1, \dots, l_t$  are radii in the disk and (ii)  $f$  maps each  $r_i$  homeomorphically to  $l_j$  for some  $j$ .*

Consider the Yin set in Figure 1(d,e). For each endpoint  $q_e$  of the horizontal or vertical yellow lines,  $\partial\mathcal{Y} \cap \overline{\mathcal{N}(q_e)}$  is *uniquely* represented as a single folded disk centered at  $q_e$  with  $k = 2$  and  $t = 1$ ; see Figure 4(b). In particular,  $\partial\mathcal{Y} \cap \overline{\mathcal{N}(q_e)}$  cannot be considered as two disks glued along a single radius at  $q_e$ : although in Figure 4(b) cutting  $\mathcal{D}$  along  $r_1$  yields two disks, but according to Definition 5.1, none of them is a disk at  $p$ . In contrast, for the intersection  $q_X$  of the horizontal and vertical yellow lines, the representation of  $\partial\mathcal{Y} \cap \overline{\mathcal{N}(q_X)}$  is far from unique: it can be represented as four disks glued along four radii at  $q_X$ , or two folded disks (with  $k = 2$  and  $t = 1$ ) glued along two radii at  $q_X$ , or a folded disk (with  $k = 4$  and  $t = 2$ ) and a disk glued along two radii at  $q_X$ , etc.

**5.4. Good pairing.** The ambiguity caused by folded disks is not conducive to the unique B-rep for Yin sets. A key notion to resolve this ambiguity is

DEFINITION 5.12 (Good pairing). *For a non-isolated non-manifold point  $p \in \partial\mathcal{Y}$ , a good pairing of sectors on a single radius  $r$  in  $\mathcal{N}(p)$  is a decomposition of these sectors into pairs such that the two set unions  $F \cup F'$  and  $G \cup G'$  of any two pairs  $(F, F')$  and  $(G, G')$  have no proper intersections, cf. Definition 4.2. The good pairings for all radii in  $\mathcal{N}(p)$  constitute a good pairing (of all sectors) within  $\mathcal{N}(p)$ .*

A good pairing of sectors on a radius  $r$  in  $\overline{\mathcal{N}(p)}$  is said to *locally bound*  $\mathcal{Y}$  if, for each pair  $(F, F')$  in the good pairing,  $F \cup F'$  is a subset of the boundary of a single maximally connected component of  $\overline{\mathcal{N}(p)} \cap \mathcal{Y}$ . A good pairing within  $\overline{\mathcal{N}(p)}$  is said to *locally bound*  $\mathcal{Y}$  if the good pairing for *each* radius in  $\overline{\mathcal{N}(p)}$  locally bounds  $\mathcal{Y}$ .

LEMMA 5.13 (Good pairing for a single radius). *For a non-manifold point  $p \in \partial\mathcal{Y}$ , the number  $n_{gp}$  of different good pairings for any radius  $r$  in  $\mathcal{N}(p)$  is either 1 or 2. For  $n_{gp} = 1$ , the good pairing locally bounds both  $\mathcal{Y}$  and  $\mathcal{Y}^\perp$ . For  $n_{gp} = 2$ , one good pairing locally bounds  $\mathcal{Y}$  while the other locally bounds  $\mathcal{Y}^\perp$ .*

*Proof.*  $n_{gp} = 1$  if there are only two sectors within  $\mathcal{N}(p)$ , i.e., if  $p$  is a vertex non-manifold point with an artificial radius  $r'$  in Convention 5.4. Otherwise Definition 5.6 implies that the number of sectors on any  $r \in \mathcal{R}(p)$  is an even number greater than 2. By Definition 5.12, two sectors form a pair if and only if they are next to each other. Hence there exist two and only two different good pairings. The rest of the proof follows from Lemma 5.5(c).  $\square$

To proceed from the good pairing for a single radius to that in the entire good neighborhood, we need

LEMMA 5.14. *For two distinct non-isolated non-manifold points  $p, q \in \partial\mathcal{Y}$ , suppose a radius  $r_1$  in  $\mathcal{N}(p)$  has a non-empty intersection with a radius  $r_2$  in  $\mathcal{N}(q)$ . Then there is a one-to-one correspondence between the sectors of  $\mathcal{N}(p)$  on  $r_1$  and sectors of  $\mathcal{N}(q)$  on  $r_2$ , where the corresponding sectors intersect in a 2D subset of  $\mathcal{N}(p) \cap \mathcal{N}(q)$ .*

*Proof.* Let  $x \in \mathcal{N}(p)$  be a point in  $r_1 \cap r_2$ . Consider a good disk decomposition of a good neighborhood  $\mathcal{N}(x)$ . By making  $\mathcal{N}(x)$  sufficiently small, we can assume

that  $\mathcal{N}(x)$  is contained in both  $\mathcal{N}(p)$  and  $\mathcal{N}(q)$ . Note that  $\mathcal{N}(x)$  has only two radii, each of which is a subset of  $r_1 \cap r_2$  as long as we make  $\mathcal{N}(x)$  small enough. Each sector in  $\mathcal{N}(x)$  is contained in a sector of  $\mathcal{N}(p)$  on  $r_1$  and each sector of  $\mathcal{N}(p)$  on  $r_1$  contains exactly one sector of  $\mathcal{N}(x)$ . A similar statement holds for sectors in  $\mathcal{N}(x)$  and  $\mathcal{N}(q)$ . Therefore, there is a natural one-one correspondence between sectors in  $\mathcal{N}(p)$  and  $\mathcal{N}(q)$  in that the corresponding pair contains the same sector of  $\mathcal{N}(x)$ .  $\square$

So long as  $\mathcal{N}(p)$  and  $\mathcal{N}(q)$  are good neighborhoods, the two distinct non-manifold points  $p, q$  in Lemma 5.14 can be both vertex non-manifold, or both non-vertex non-manifold, or one vertex non-manifold and the other non-vertex non-manifold.

LEMMA 5.15 (Good pairings in a good neighborhood of a non-manifold point).

*For any non-manifold point  $p \in \partial\mathcal{Y}$ , the number  $n_{gp}$  of different good pairings in  $\mathcal{N}(p)$  is either 1 or 2. If  $n_{gp} = 1$ , the good pairing locally bounds both  $\mathcal{Y}$  and  $\mathcal{Y}^\perp$ . If  $n_{gp} = 2$ , one good pairing locally bounds  $\mathcal{Y}$  while the other locally bounds  $\mathcal{Y}^\perp$ .*

*Proof.* First, we consider the case of  $p$  being non-vertex non-manifold. By Definitions 3.4 and 5.2,  $\mathcal{N}(p)$  has exactly two radii  $r_1$  and  $r_2$  intersecting only at  $p$  and the number of sectors on each of the two radii is  $2n$  where  $n > 1$ . Choose two non-vertex non-manifold points  $q_1 \in r_1$ ,  $q_2 \in r_2$  and two good neighborhoods  $\mathcal{N}(q_1)$ ,  $\mathcal{N}(q_2)$  so that  $\mathcal{N}(q_1) \subset \mathcal{N}(p)$ ,  $\mathcal{N}(q_2) \subset \mathcal{N}(p)$ , and  $\mathcal{N}(q_1) \cap \mathcal{N}(q_2) \neq \emptyset$ . Then the conclusion follows from Lemma 5.14.

Hereafter we consider the case of  $p$  being vertex non-manifold.

Suppose  $\overline{\mathcal{N}(p)} \cap \partial\mathcal{Y}$  can be uniquely represented as a folded disk with  $t = 1$ , cf. the example under Definition 5.11 with  $k = 2$  and  $t = 1$ . Then by Definition 5.11, all sectors share the common radius  $l_1$ . By Convention 5.4, all other radii are artificial. Therefore there is only one good pairing of these sectors.

Otherwise  $\overline{\mathcal{N}(p)} \cap \partial\mathcal{Y}$  is either a folded disk with  $t > 1$  or not a folded disk. In both cases, Lemma 5.10 dictates that the set  $\mathcal{I}$  of all non-isolated non-manifold points is a 1D CW complex homeomorphic to a graph  $G = (V, E, \phi_G)$ , where  $V$  is the set of all vertex non-manifold points and  $E$  that of curves connecting points in  $V$ . Choose a set  $P := \{p_1, p_2, \dots, p_m\}$  of points in  $E$  and a good neighborhood for each point in  $P \cup V$  such that these good neighborhoods cover  $\mathcal{I}$  and the intersection of any two good neighborhoods is either the empty set or a 3-manifold. Then the proof is completed by applying Lemma 5.14 to all pairs of intersecting good neighborhoods.  $\square$

**5.5. Good disk decomposition.** Lemma 5.13 leads to another characterization of the local topology of a non-manifold point in terms of disks and folded disks.

LEMMA 5.16. *For a non-manifold point  $p \in \partial\mathcal{Y}$ , the 2D subset  $\partial\mathcal{Y} \cap \overline{\mathcal{N}(p)}$  is the union of a finite number of disks and folded disks, no pair of which intersect properly. In particular,  $p$  being non-vertex non-manifold implies that  $\partial\mathcal{Y} \cap \overline{\mathcal{N}(p)}$  is the union of a finite number of disks, each of which is the union of a good pair of sectors.*

*Proof.* By Lemma 5.13, for each  $r \in \mathcal{R}(p)$ , we always have a good pairing of sectors on  $r$ . Then the sectors can be arranged to form disks or folded disks: for any initial sector  $F_0$ , the pairing gives a unique sequence of sectors  $F_0, F_1, \dots, F_{k-1}, F_k = F_0$ , where each sector  $F_i$  is on radii  $r_i$  and  $r_{i+1}$ , the paired sectors  $F_i$  and  $F_{i+1}$  in the given good pairing satisfies  $r_{i+1} = F_i \cap F_{i+1}$ , and  $F_i \neq F_j$  holds unless  $\{i, j\} = \{0, k\}$ . As one goes from  $F_0$  to  $F_k$ , if there exists one radius which is passed twice, then  $\bigcup_{0 \leq i \leq k} F_i$  is a folded disk. Otherwise  $\bigcup_{0 \leq i \leq k} F_i$  is a disk. By construction, these disks and folded disks intersect only at radii. By Definition 5.12, no pair of these disks intersect properly. Finally, if  $p$  is non-vertex non-manifold, Definition 5.11 dictates that  $\mathcal{N}(p)$

cannot contain any folded disks.  $\square$

Lemma 5.16 guarantees the existence of

DEFINITION 5.17 (Good disk decomposition). *For a non-manifold point  $p \in \partial\mathcal{Y}$ , a good disk decomposition of  $\partial\mathcal{Y} \cap \overline{\mathcal{N}(p)}$  is a finite set  $\mathbf{D}(p) := \{\mathcal{D}_i : i = 1, 2, \dots, m\}$  of disks and/or folded disks such that  $\partial\mathcal{Y} \cap \overline{\mathcal{N}(p)}$  coincides with*

$$(5.2) \quad \mathcal{U}(\mathbf{D}(p)) := \cup_{\mathcal{D}_i \in \mathbf{D}(p)} \mathcal{D}_i$$

where no pairs of disks in  $\mathbf{D}(p)$  intersect properly and the improper intersection of any two distinct disks is either  $p$  or a finite number of radii in  $\mathcal{R}(p)$ .

DEFINITION 5.18 (Locally bound). *A good disk decomposition  $\mathbf{D}(p)$  of  $\partial\mathcal{Y} \cap \overline{\mathcal{N}(p)}$  is said to locally bound  $\mathcal{Y}$  or  $\mathcal{Y}^\perp$  if, for any  $\mathcal{D}_i \in \mathbf{D}(p)$ , each sector pair in  $\mathcal{D}_i$  is in some good pairing within  $\mathcal{N}(p)$  that locally bounds  $\mathcal{Y}$  or  $\mathcal{Y}^\perp$ , respectively.*

The uniqueness of the good disk decomposition locally bounding  $\mathcal{Y}$  is stated in

COROLLARY 5.19 (Good disk decomposition of a good neighborhood). *For a non-manifold point  $p \in \partial\mathcal{Y}$ , the number  $n_{dd}$  of different good disk decompositions of  $\mathcal{N}(p)$  is either 1 or 2. If  $n_{dd} = 1$ , the good disk decomposition locally bounds both  $\mathcal{Y}$  and  $\mathcal{Y}^\perp$ . If  $n_{dd} = 2$ , the good disk decomposition locally bounds  $\mathcal{Y}$  while the other locally bounds  $\mathcal{Y}^\perp$ .*

*Proof.* This follows from Lemma 5.15 and Definitions 5.17 and 5.18.  $\square$

For the Yin set in Figure 1(d,e), we have  $n_{dd} = 1$  for the endpoints of both the horizontal and vertical yellow lines and  $n_{dd} = 2$  for their intersection  $q_X$ .

**6. Global topology.** To proceed from local topology to global topology in Theorem 6.3, we need two operations on non-manifold points, one for non-vertex points in Definition 6.1 and the other for isolated points in Definition 6.2.

By Definition 3.4, the good neighborhood of a non-vertex non-manifold point  $p$  has two and only two radii  $r_1$  and  $r_2$ . A good disk decomposition  $\mathbf{D}(p)$  has no folded disks but disks, whose common intersection is  $r = r_1 \cup r_2$ .

DEFINITION 6.1 (Unfolding). *For a non-vertex non-manifold point  $p \in \partial\mathcal{Y}$ , the  $\epsilon$ -unfolding operation for a good disk decomposition  $\mathbf{D}(p)$  of  $\partial\mathcal{Y} \cap \overline{\mathcal{N}(p)}$  is a continuous function  $f : \mathcal{D}_\sqcup(p) \times [0, 1] \rightarrow \overline{\mathcal{N}(p)}$  where  $\mathcal{D}_\sqcup(p) := \sqcup_{\mathcal{D}_i \in \mathbf{D}(p)} \mathcal{D}_i$  with  $\sqcup$  given in (5.1) and*

- (a)  $f(\mathcal{D}_\sqcup(p) \times 0) = \mathcal{U}(\mathbf{D}(p))$  where  $\mathcal{U}$  is given in (5.2);
- (b) for any  $t \in (0, 1]$ , each  $\mathcal{D}_i$  and its image under  $f|_{\mathcal{D}_i \times \{t\} \times \{t\}}$  are homeomorphic;
- (c)  $f(\mathcal{D}_\sqcup(p) \times 1) = \mathcal{U}(\tilde{\mathbf{D}}(p))$ , where  $\tilde{\mathbf{D}}(p) = \{\tilde{\mathcal{D}}_i\}$  is a new set of disks such that (i) the restriction  $f|_{\partial\mathcal{D}_i \times \{t\} \times \{t\}}$  is an identity where  $\partial\mathcal{D}_i$  is defined in Definition 5.1, (ii)  $\tilde{\mathcal{D}}_i \cap \mathcal{N}(p)$ 's are pairwise disjoint, (iii) the disks in  $\tilde{\mathbf{D}}(p)$  have a one-to-one correspondence to those in  $\mathbf{D}(p)$  and, (iv) the maximal distance of corresponding points in  $\mathcal{U}(\mathbf{D}(p))$  and  $\mathcal{U}(\tilde{\mathbf{D}}(p))$  is no greater than  $\epsilon$ .

The above unfolding operation is well defined since there always exists a function  $f$  that continuously deforms each disk  $\mathcal{D}_i$  to  $\tilde{\mathcal{D}}_i$  in  $\mathbb{R}^3$ . Furthermore, the unfolding can be performed one disk at a time so that no new intersections are introduced; it can also be confined within an arbitrarily small neighborhood of the radius  $r$  so that the max-norm error of approximating each  $\mathcal{D}_i$  with  $\tilde{\mathcal{D}}_i$  is no greater than  $\epsilon$ . Consequently, the unfolding operation eliminates all non-vertex non-manifold points in  $\mathcal{N}(p)$ , except those on  $\partial\mathcal{N}(p)$ . To understand (c)(i), consider a vertex non-manifold point  $p_v$  of the

Yin set  $\mathcal{Y}$  in Figure 1(b) and a good neighborhood  $\mathcal{N}(q)$  of a non-vertex non-manifold point  $q$  close to  $p_v$ . For  $\mathcal{N}(q)$  satisfying  $p_v \in \partial\mathcal{N}(q)$ , we *cannot* separate  $p_v$  into multiple points because  $p_v$  is the *single* center of a folded disk. Indeed, a folded disk in  $\mathcal{N}(q)$  should be transformed to a disk.

**DEFINITION 6.2** (Detaching). *For an isolated non-manifold point  $p \in \partial\mathcal{Y}$ , the  $\epsilon$ -detaching operation for a good disk decomposition  $\mathbf{D}(p)$  of  $\partial\mathcal{Y} \cap \overline{\mathcal{N}(p)}$  is a continuous map  $f : \mathcal{D}_\square(p) \times [0, 1] \rightarrow \overline{\mathcal{N}(p)}$  satisfying (a,b,c) in Definition 6.1.*

Different from those in Definition 6.1,  $\partial\mathcal{D}_i$ 's of  $\mathbf{D}(p)$  in Definition 6.2 are pairwise disjoint and thus condition (c)(ii) implies that the disks in  $\mathbf{D}(p)$  are pairwise disjoint. In addition, the sequential perturbation of detaching one disk at a time is confined within an arbitrarily small neighborhood of  $p$  since there are no radii in  $\mathcal{N}(p)$ .

**THEOREM 6.3** (Global topology of 3D Yin sets). *The boundary of any Yin set  $\mathcal{Y} \neq \emptyset, \mathbb{R}^3$  is homeomorphic to the gluing of a finite collection of surfaces along a 1D CW complex.*

*Proof.* By Lemma 5.10(b), the non-manifold points of  $\partial\mathcal{Y}$  form a 1D CW complex. Consider a maximally connected component  $l$  of this 1D CW complex. If  $l$  only consists of a single isolated non-manifold point, the conclusion holds trivially. Otherwise denote by  $V$  the set of all vertex non-manifold points in  $l$ . It is straightforward to select a set  $P = \{p_i \in l : i = 1, 2, \dots, m\}$  of non-vertex non-manifold points and a good neighborhood for each point in  $P$  such that

- (a)  $i \neq j \implies p_i \notin \mathcal{N}(p_j)$ , i.e.,  $p_i$  is contained only in  $\mathcal{N}(p_i)$ ;
- (b)  $v \in V \implies v \notin \cup_{i=1}^m \mathcal{N}(p_i)$ ;
- (c) for each radius  $r$  at  $v \in V$ ,  $v \in \partial\mathcal{N}(p_i)$  and  $(r \setminus v) \subset \mathcal{N}(p_i)$  hold for some  $p_i \in P$ ;
- (d)  $l \subset \cup_{i=1}^m \overline{\mathcal{N}(p_i)}$ .

(b) states that no vertex non-manifold point is contained in any of the good neighborhoods while (c) states that each non-vertex non-manifold point in  $\mathcal{N}(v)$  is contained in some  $\mathcal{N}(p_i)$ ; together they imply  $(l \setminus V) \subset \cup_{i=1}^m \mathcal{N}(p_i)$ . See Figure 5 for an example of selecting  $P$  and good neighborhoods of points in  $P$ . By Corollary 5.19, for each  $\mathcal{N}(p_i)$  and each  $\mathcal{N}(v)$ , the good disk decomposition that locally bounds  $\mathcal{Y}$  is unique. By (d) and Lemma 5.14, any two adjacent disk decompositions, either non-vertex/non-vertex or vertex/non-vertex, are compatible.

By Definition 6.1, the application of the unfolding operation to each good disk decomposition in  $\mathcal{N}(p_i)$  eliminates all non-vertex non-manifold point of  $\mathcal{Y}$ . It also converts each vertex non-manifold point of  $l$  to either an isolated non-manifold point or a manifold point; an example of the latter case is some  $v \in V$  where the good disk decomposition of  $\mathcal{N}(v)$  only consists of folded disks. Now that all non-manifold points of  $\partial\mathcal{Y}$  are isolated, the application of the detaching operation in Definition 6.2 to the good disk decomposition in the good neighborhood of each isolated non-manifold point yields a surface in Definition 4.1.

Apply the above process to each connected component of non-manifold points of  $\partial\mathcal{Y}$  and we obtain a finite number of surfaces. Denote by  $\partial\tilde{\mathcal{Y}}$  the resulting space, where each point  $p \in \partial\tilde{\mathcal{Y}}$  has a neighborhood homeomorphic to an open disk in  $\mathbb{R}^2$ . Since  $\partial\mathcal{Y}$  is compact,  $\partial\tilde{\mathcal{Y}}$  is also compact. Therefore  $\partial\tilde{\mathcal{Y}}$  is the union of a finite number of disjoint surfaces. Finally, the unfolding and detaching operations can be undone by first gluing at points in  $V$  and then gluing along the edges in the 1D CW complex.  $\square$

**7. Boundary representation.** Theorem 6.3 leads to a unique B-rep of Yin sets in Theorem 7.10, which states that the boundary of a 3D Yin set can be uniquely

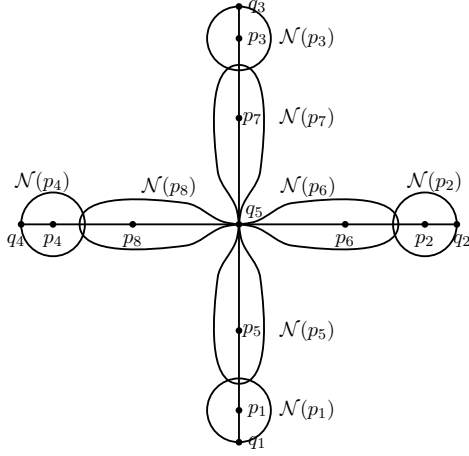


FIG. 5. Illustrating the proof of Theorem 6.3 with the Yin set  $\mathcal{Y}$  in Figure 1(d,e). Each point in  $\{q_i : i = 1, 2, 3, 4, 5\}$  is a vertex non-manifold point of  $\mathcal{Y}$  while each point in  $\{p_i : i = 1, \dots, 8\}$  is a selected non-vertex non-manifold point. For each  $i = 1, 2, 3, 4$ , we have  $q_i \in \partial N(p_i)$  and  $q_i \notin N(p_i)$ ; the fact of  $N(p_i) \cap N(p_{i+4}) \neq \emptyset$  implies the compatibility of their good disk decompositions. For each  $j = 5, 6, 7, 8$ , we have  $q_5 \in \partial N(p_j)$  and  $q_5 \notin N(p_j)$ ; the fact of  $N(p_j) \cap N(q_5) \neq \emptyset$  implies the compatibility of the good disk decomposition in  $N(q_5)$  with that in each  $N(p_j)$ .

decomposed into a collection of basic building blocks called glued surfaces.

DEFINITION 7.1 (Glued surface). A glued surface is a quotient space of a surface such that (i) the quotient map glues the surface along a 1D CW complex, and (ii) the complement of the glued surface in  $\mathbb{R}^3$  has exactly two connected components, one bounded and the other unbounded.

Condition (i) identifies the orientation of a glued surface with that of the original surface while condition (ii) preserves the key property that the original surface has a bounded complement and an unbounded complement in  $\mathbb{R}^3$ , which is crucial in the unique boundary representation of Yin sets. Then Definitions 4.2, 4.4, and 4.5 generalize to glued surfaces in a straightforward manner.

DEFINITION 7.2 (Almost disjoint glued surfaces). Two glued surfaces are almost disjoint if they have no proper intersections and their improper intersections, cf. Definition 4.2, only consist of a finite number of isolated points and disjoint curves.

DEFINITION 7.3 (Orientations of a glued surface). A glued surface is positively oriented if the normal vector  $\mathbf{n}$  of the original surface always points from its bounded complement to its unbounded complement; otherwise it is negatively oriented.

DEFINITION 7.4 (Internal complement of a glued surface). The internal complement of a glued surface  $\mathcal{S}$ , written  $\text{int}(\mathcal{S})$ , is its bounded complement if  $\mathcal{S}$  is positively oriented; otherwise it is the unbounded complement.

The external complement of a glued surface  $\mathcal{S}$  is the connected component of  $\mathbb{R}^3 \setminus \mathcal{S}$  that is not  $\text{int}(\mathcal{S})$ .

DEFINITION 7.5 (Inclusion of glued surfaces). A glued surface  $\mathcal{S}_k$  is said to include  $\mathcal{S}_l$ , written  $\mathcal{S}_k \geq \mathcal{S}_l$  or  $\mathcal{S}_l \leq \mathcal{S}_k$ , if and only if the bounded complement of  $\mathcal{S}_l$  is a subset of that of  $\mathcal{S}_k$ . If  $\mathcal{S}_k$  includes  $\mathcal{S}_l$  and  $\mathcal{S}_k \neq \mathcal{S}_l$ , we write  $\mathcal{S}_k > \mathcal{S}_l$  or  $\mathcal{S}_l < \mathcal{S}_k$ .

Equipped with the above partial ordering, any collection of glued surfaces can be

considered as a partially ordered set (poset) of glued surfaces.

**DEFINITION 7.6** (Covering of glued surfaces). *Let  $\mathcal{G}$  denote a poset of glued surfaces with inclusion as the partial order. We say  $\mathcal{S}_k$  covers  $\mathcal{S}_l$  in  $\mathcal{G}$  and write " $\mathcal{S}_k \succ \mathcal{S}_l$ " or " $\mathcal{S}_l \prec \mathcal{S}_k$ " if  $\mathcal{S}_l < \mathcal{S}_k$  and no elements  $\mathcal{S} \in \mathcal{G}$  satisfy  $\mathcal{S}_l < \mathcal{S} < \mathcal{S}_k$ .*

**DEFINITION 7.7** (Glued-surface decomposition). *A glued-surface decomposition of the boundary of a connected Yin set  $\mathcal{Y} \neq \emptyset, \mathbb{R}^3$  is a poset  $\mathcal{G}_{\partial\mathcal{Y}} = \{\mathcal{S}_j\}$  of pairwise almost disjoint glued surfaces such that  $\partial\mathcal{Y} = \cup_{\mathcal{S}_j \in \mathcal{G}_{\partial\mathcal{Y}}} \mathcal{S}_j$ .*

By Lemma 5.10(b), the set  $Q$  of all non-manifold points of  $\partial\mathcal{Y}$  form a 1D CW complex homeomorphic to a graph  $G = (V, E, \phi_G)$ , where each vertex  $v \in V$  is either an isolated non-manifold point or a vertex non-manifold point of  $\partial\mathcal{Y}$  and  $E$  contains the curves as the maximally connected subsets of  $Q \setminus V$ .

**DEFINITION 7.8** (Algorithm of glued-surface decomposition). *Given a connected Yin set  $\mathcal{Y} \neq \emptyset, \mathbb{R}^3$  and the graph  $G = (V, E, \phi_G)$  homeomorphic to the 1D CW complex of non-manifold points on  $\partial\mathcal{Y}$ , the algorithm of glued-surface decomposition is the following sequence of steps that construct a finite collection  $\mathcal{G}_{\partial\mathcal{Y}}$  of 2D subsets of  $\mathbb{R}^3$ .*

*Firstly, we decompose  $\partial\mathcal{Y}$  to a set  $\mathcal{G}_{cc}$  of surfaces and surfaces with boundary.*

- (CC.1) *For each isolated non-manifold point  $p \in V$ , apply the detaching operation in Definition 6.2 to the good disk decomposition in  $\mathcal{N}(p)$ .*
- (CC.2) *For each curve  $\gamma \in E$  with  $m > 2$  sectors on it, cut  $\partial\mathcal{Y}$  open along  $\gamma$ , i.e., replace  $\gamma$  with  $m$  pairwise disjoint curves  $\gamma_1, \gamma_2, \dots, \gamma_m$  so that, for any  $i \neq j$ , the  $i$ th and the  $j$ th sectors on  $\gamma$  are now on disjoint radii  $\gamma_i$  and  $\gamma_j$ .*
- (CC.3) *Each maximally connected component of  $\partial\tilde{\mathcal{Y}}$  that results from (CC.2) is either a surface or a surface with boundary, because all non-manifold points have been removed. Hereafter we denote by  $\mathcal{G}_{cc}$  the set of these components.*

*Second, we initialize  $\mathcal{G}_{\partial\mathcal{Y}}$  with all glued surfaces in  $\mathcal{G}_{cc}$ , remove them from  $\mathcal{G}_{cc}$ , and write  $\mathcal{G}_{cc} = \{P_j\}$  where each  $P_j$  is a surface with boundary.*

*Lastly, we finish the construction of  $\mathcal{G}_{\partial\mathcal{Y}}$  by steps as follows.*

- (GS.1) *Form a connected 2D subset  $P_{GS}$  (with empty boundary) from  $\mathcal{G}_{cc}$ :*
  - (a) *remove an arbitrary  $P_j \in \mathcal{G}_{cc}$  from  $\mathcal{G}_{cc}$  as the starting point;*
  - (b) *locate a boundary curve  $\gamma \subset \partial P_j$  and find the unique  $P_i \in \mathcal{G}_{cc}$  satisfying that  $(P_i, P_j)$  is a good pair on  $\gamma$  and locally bounds  $\mathcal{Y}$ ;*
  - (c) *glue  $P_i$  to  $P_j$  along  $\gamma$ , remove  $P_i$  from  $\mathcal{G}_{cc}$ , and update  $P_j$  with  $P_i \cup P_j$ ;*
  - (d) *repeat (b,c) until the boundary of  $P_j$  becomes empty and set  $P_{GS} = P_j$ .*
- (GS.2) *Decompose  $P_{GS}$  into a finite collection  $\mathbf{S}_{GS} = \{\mathcal{S}_j\}$  of 2D subsets of  $\mathbb{R}^3$ :*
  - (a) *cut  $P_{GS}$  open along curves in  $E$  in the same way as that of (CC.2) to obtain a collection of surfaces with boundary;*
  - (b) *glue these surfaces with boundary to form  $\mathbf{S}_{GS}$ , a collection of 2D subsets with empty boundary, by the same substeps in (GS.1a-d) except that here a good pairing  $(P_i, P_j)$  on  $\gamma$  is required to locally bound  $\mathcal{Y}^\perp$  instead of  $\mathcal{Y}$ ;*
- (GS.3) *Update  $\mathcal{G}_{\partial\mathcal{Y}}$  with  $\mathcal{G}_{\partial\mathcal{Y}} \cup \mathbf{S}_{GS}$ ;*
- (GS.4) *Repeat (GS.1-3) until  $\mathcal{G}_{cc}$  is empty.*

We emphasize that the steps (GS.2-4) are necessary because  $P_{GS}$  needs not to be a glued surface; see the example shown in Figure 6 to illustrate Definition 7.8.

**LEMMA 7.9** (Unique glued-surface decomposition of 3D Yin sets). *For any connected Yin set  $\mathcal{Y} \neq \emptyset, \mathbb{R}^3$ , the output  $\mathcal{G}_{\partial\mathcal{Y}}$  of the algorithm in Definition 7.8 is the unique glued-surface decomposition of  $\partial\mathcal{Y}$  as in Definition 7.7.*

*Proof.* We need to prove (i) the construction of  $\mathcal{G}_{\partial\mathcal{Y}}$  is unique, (ii) each  $\mathcal{S}_j \in \mathcal{G}_{\partial\mathcal{Y}}$

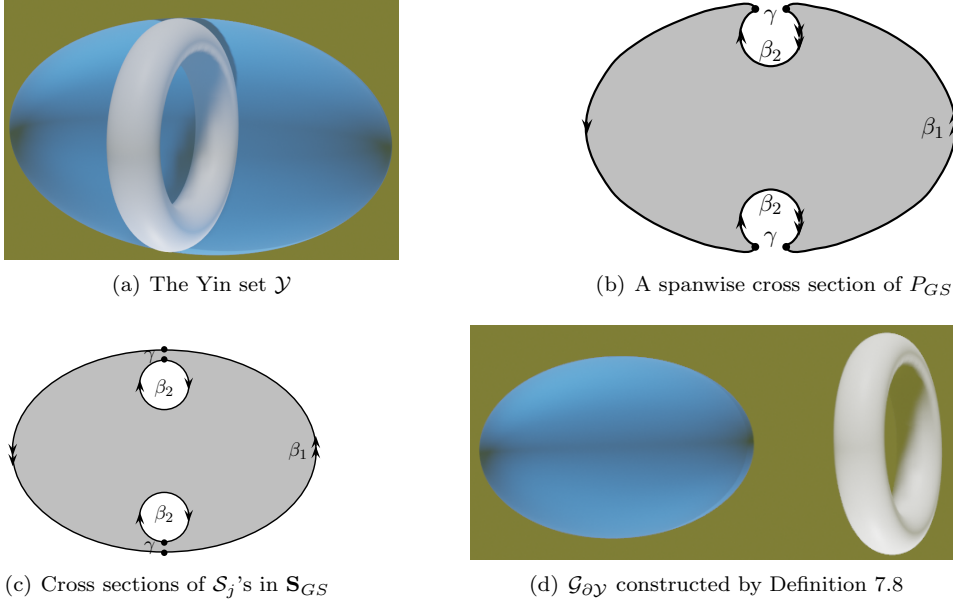


FIG. 6. Illustrating the algorithm of glued-surface decomposition in Definition 7.8. The Yin set  $\mathcal{Y}$  is obtained by removing a solid torus from an elliptical ball so that all non-manifold points on  $\partial\mathcal{Y}$  form a Jordan curve, which is also the only (improper) intersection of the ellipsoid and the torus. After the execution of (CC.1–3),  $\mathcal{G}_{cc}$  contains three surfaces with boundary  $P_1, P_2, P_c$ , where  $P_1$  and  $P_2$  are homeomorphic to the unit half sphere and  $P_c$  to the cylinder  $\mathbb{S}^1 \times [0, 1]$ . Before (GS.1),  $\mathcal{G}_{\partial\mathcal{Y}}$  is still empty because (CC.1–3) yield no glued surfaces. If the half sphere  $P_1$  is chosen as the starting point in (GS.1a), then  $P_{GS}$  is formed as  $P_1 \leftrightarrow P_c \leftrightarrow P_2$  where  $\leftrightarrow$  denotes the gluing. As shown in subplot (b),  $\mathbb{R}^3 \setminus P_{GS}$  has three connected components, two bounded and one unbounded. In (GS.2),  $P_{GS}$  is decomposed into two 2D subsets with empty boundary, whose cross sections are shown in subplot (c). They turn out to be the two surfaces shown in subplot (d).

is a glued surface, and (iii) the glued surfaces in  $\mathcal{G}_{\partial\mathcal{Y}}$  are pairwise almost disjoint.

(i) follows from the uniqueness of the algorithmic steps in Definition 7.8. In particular, the uniqueness of (GS.1b) and that of (GS.2b) follow from Lemma 5.13.

To prove (ii), we start by observing that each element in  $\mathcal{G}_{cc}$  is either a surface or a surface with boundary. Although  $P_{GS}$  produced by (GS.1) has no boundary, it may violate condition (ii) in Definition 7.1 and thus fail to be a glued surface. Nonetheless, by  $\mathcal{S}_j \subset P_{GS} \subset \partial\mathcal{Y}$ , the condition of locally bounding  $\mathcal{Y}$  in (GS.1b), and the connectedness of  $\mathcal{Y}$ , one and *only* one connected component  $C_{\mathcal{Y}}$  of  $\mathbb{R}^3 \setminus P_{GS}$  contains  $\mathcal{Y}$ . By Lemma 5.5(c),  $\partial\mathcal{Y} \setminus \mathcal{S}_j$  must also be contained in  $C_{\mathcal{Y}}$ . On the other hand,  $\mathcal{Y}^\perp$  cannot be distributed in multiple connected components of  $\mathbb{R}^3 \setminus \mathcal{S}_j$  other than  $C_{\mathcal{Y}}$ , because that would contradict the condition of locally bounding  $\mathcal{Y}^\perp$  in (GS.2b). For any point  $p \notin \mathcal{S}_j$ , one and only one of  $p \in \mathcal{Y}$ ,  $p \in \mathcal{Y}^\perp$ , and  $p \in \partial\mathcal{Y} \setminus \mathcal{S}_j$  holds. Therefore,  $\mathbb{R}^3 \setminus \mathcal{S}_j$  only consists of two components, one containing  $\mathcal{Y}$  and the other being contained in  $\mathcal{Y}^\perp$ . Thus by Definition 7.1  $\mathcal{S}_j$  is indeed a glued surface.

(iii) follows from Definition 7.2 and the fact of all improper intersections of the glued surfaces being preserved, i.e., each detaching or cutting-open operation is matched with a gluing operation.  $\square$

The main result of this section is

**THEOREM 7.10** (Unique B-rep of connected Yin sets). *The boundary  $\partial\mathcal{Y}$  of*

any connected Yin set  $\mathcal{Y} \neq \emptyset, \mathbb{R}^3$  can be uniquely decomposed into a finite poset  $\mathcal{G}_{\partial\mathcal{Y}} = \{\mathcal{S}_j \subset \partial\mathcal{Y}\}$  of pairwise almost disjoint oriented glued surfaces such that

$$(7.1) \quad \mathcal{Y} = \bigcap_{\mathcal{S}_j \in \mathcal{G}_{\partial\mathcal{Y}}} \text{int}(\mathcal{S}_j).$$

Furthermore, the poset  $\mathcal{G}_{\partial\mathcal{Y}}$  must be one of the following two types,

$$(7.2) \quad \begin{cases} \mathcal{G}^- = \{\mathcal{S}_1^-, \mathcal{S}_2^-, \dots, \mathcal{S}_{n_-}^-\}, & n_- \geq 1, \\ \mathcal{G}^+ = \{\mathcal{S}^+, \mathcal{S}_1^-, \mathcal{S}_2^-, \dots, \mathcal{S}_{n_-}^-\}, & n_- \geq 0, \end{cases}$$

where all  $\mathcal{S}_j^-$ 's are negatively oriented and mutually incomparable with respect to inclusion. For  $\mathcal{G}^+$ , we also have

$$(7.3) \quad \forall j = 1, 2, \dots, n_-, \quad \mathcal{S}_j^- \prec \mathcal{S}^+.$$

*Proof.* By Lemma 7.9, the poset  $\mathcal{G}_{\partial\mathcal{Y}}$  is the unique decomposition of  $\partial\mathcal{Y}$ . For each  $\mathcal{S}_j \in \mathcal{G}_{\partial\mathcal{Y}}$ , we orient it according to Definitions 7.3 and 7.4 so that the internal complement of  $\mathcal{S}_j$  always contains  $\mathcal{Y}$ . For example, in Figure 6(d) the ellipsoid is positively oriented while the torus is negatively oriented.

The connectedness of  $\mathcal{Y}$  implies that  $\mathcal{Y}$  is contained in a single complement of each  $\mathcal{S}_j$ . By Definition 7.1,  $\mathbb{R}^3 \setminus \mathcal{S}_j$  only has two connected components and we have  $\mathcal{Y} \subset \text{int}(\mathcal{S}_j)$  for each  $\mathcal{S}_j \in \mathcal{G}_{\partial\mathcal{Y}}$ . Then  $\partial\mathcal{Y} = \cup_j \mathcal{S}_j$  gives (7.1).

Suppose  $\mathcal{G}_{\partial\mathcal{Y}}$  has two or more positively oriented glued surfaces  $\mathcal{S}_1$  and  $\mathcal{S}_2$ . Then Definition 7.4 implies that both bounded complements of  $\mathcal{S}_1$  and  $\mathcal{S}_2$  are subsets of  $\mathcal{Y}$ , which contradicts  $\mathcal{Y}$  being entirely contained in only one complement of each  $\mathcal{S}_j$ .

If  $\mathcal{G}_{\partial\mathcal{Y}}$  has no positively oriented glued surfaces,  $\mathcal{Y} \neq \emptyset$  dictates that at least one negatively oriented glued surface exists in  $\mathcal{G}_{\partial\mathcal{Y}}$  and thus  $\mathcal{G}_{\partial\mathcal{Y}}$  must be of the  $\mathcal{G}^-$  type. If  $n_- = 1$ , (7.2) holds trivially. For  $n_- > 1$ , any two glued surfaces  $\mathcal{S}_1^-$  and  $\mathcal{S}_2^-$  must be incomparable; otherwise it would contradict the connectedness of  $\mathcal{Y}$ .

If  $\mathcal{G}_{\partial\mathcal{Y}}$  has one positively oriented glued surfaces, then  $\mathcal{G}_{\partial\mathcal{Y}}$  must be of the  $\mathcal{G}^+$  type. If  $n_- = 0$ , (7.2) and (7.3) hold trivially. For  $n_- > 0$ , suppose (7.3) did not hold for some negatively oriented glued surface  $\mathcal{S}_1^-$ . Then  $\mathcal{S}_1^- \succ \mathcal{S}^+$  or they are incomparable. For the former case, a path from one point in the internal complement of  $\mathcal{S}_1^-$  to another point in the internal complement of  $\mathcal{S}^+$  must contain some points not in  $\mathcal{Y}$ , and this contradicts the connectedness of  $\mathcal{Y}$ . The latter case also contradicts the connectedness of  $\mathcal{Y}$ . Thus (7.3) holds. In addition, arguments similar to those in the previous paragraph imply that the negatively oriented glued surfaces are pairwise incomparable.  $\square$

Theorem 7.10 is applied to each connected component of a general Yin set to get

**COROLLARY 7.11** (Unique B-rep of Yin sets). *For any Yin set  $\mathcal{Y} \neq \emptyset, \mathbb{R}^3$ , its boundary  $\partial\mathcal{Y}$  can be uniquely decomposed into a collection*

$$(7.4) \quad \mathcal{G}_{\partial\mathcal{Y}} = \{\mathcal{G}_i = \{\mathcal{S}_{i,j} \subset \partial\mathcal{Y}_i\} : \mathcal{Y}_i \text{ is a connected component of } \mathcal{Y}\}$$

*of posets of pairwise almost disjoint oriented glued surfaces such that*

$$(7.5) \quad \mathcal{Y} = \bigcup_i^{\perp\perp} \bigcap_j \text{int}(\mathcal{S}_{i,j}),$$

*where each  $\mathcal{G}_i$  satisfies Theorem 7.10.*

**8. Conclusion.** We have proposed the Yin space as a model of 3D continua with arbitrarily complex topology. In particular, we have characterized the local and global topology of singular points on the boundary of a 3D Yin set. The main theorem on the global topology of 3D Yin sets also leads to their unique B-rep via glued surfaces. This work is our first step of 3D fluid modeling in the study of multiphase flows.

Several future research prospects follow. By Theorems 6.3 and 7.10 and the fact that all compact 2-manifolds can be triangulated, it suffices to employ a simplicial 2-complex as the underlying data structure for the B-rep and 3D IT of any 3D continua. Such a linear MARS for 3D IT is already done [17] and the development of fourth- and higher-order IT methods is currently a work in progress. Other interesting topics of IT for deforming 3D continua are the theoretical characterizations and algorithmic treatments of topological changes. Finally, to integrate CAD to CAE, we will equip the 3D Yin space with a Boolean algebra so that the discretization of spatial operators in numerically solving partial differential equations can benefit from the explicit modeling of topology and geometry.

**Acknowledgments.** We acknowledge helpful comments from Shaozhen Cao, Junxiang Pan, and Chenhao Ye, graduate students at the school of mathematical sciences in Zhejiang University.

#### REFERENCES

- [1] M. ATTENE, M. CAMPEN, AND L. KOBBELT, *Polygon mesh repairing: An application perspective*, ACM Comput. Surv., 45 (2013), <https://doi.org/10.1145/2431211.2431214>.
- [2] F. BERNARDINI AND H. RUSHMEIER, *The 3D model acquisition pipeline*, Computer Graphics Forum, 21 (2002), pp. 149–172, <https://onlinelibrary.wiley.com/doi/abs/10.1111/1467-8659.00574>.
- [3] B. CAO, J. CHEN, Z. HUANG, AND Y. ZHENG, *CAD/CAE integration framework with layered software architecture*, in 2009 11th IEEE International Conference on Computer-Aided Design and Computer Graphics, 2009, pp. 410–415.
- [4] R. FAROUKI, *Closing the gap between CAD model and downstream application*, SIAM News 32, 5 (1999), pp. 303–319.
- [5] S. GIVANT AND P. HALMOS, *Introduction to Boolean Algebras*, Springer, 2009.
- [6] A. GUEZIEC, G. TAUBIN, F. LAZARUS, AND B. HOM, *Cutting and stitching: converting sets of polygons to manifold surfaces*, IEEE Transactions on Visualization and Computer Graphics, 7 (2001), pp. 136–151, <https://doi.org/10.1109/2945.928166>.
- [7] G. GUJARATHI AND Y.-S. MA, *Parametric CAD/CAE integration using a common data model*, Journal of Manufacturing Systems, 30 (2011), pp. 118–132, <https://doi.org/https://doi.org/10.1016/j.jmsy.2011.01.002>.
- [8] C. W. HIRT AND B. D. NICHOLS, *Volume of fluid (VOF) method for the dynamics of free boundaries*, J. Comput. Phys., 39 (1981), pp. 201–225.
- [9] T. IGARASHI, S. MATSUOKA, AND H. TANAKA, *Teddy: a sketching interface for 3D freeform design*, in ACM SIGGRAPH 2006 Courses, 2006, <https://doi.org/10.1145/1185657.1185772>.
- [10] X. JIA, F. CHEN, AND S. YAO, *Singularity computation for rational parametric surfaces using moving planes*, ACM Trans. Graph., 42 (2022), <https://doi.org/10.1145/3551387>.
- [11] C. JORDAN, *Cours D’Analyse l’École Polytechnique*, Paris, 1887. pp. 587–594.
- [12] M. T. H. KHAN AND S. REZWANA, *A review of CAD to CAE integration with a hierarchical data form (HDF)-based solution*, Journal of King Saud University – Engineering Sciences, 33 (2021), pp. 248–258. <https://doi.org/10.1016/j.jksues.2020.04.009>.
- [13] K. LI, X. JIA, AND F. CHEN, *Fast determination and computation of self-intersections for NURBS surfaces*, ACM Trans. Graph., 44 (2025), <https://doi.org/10.1145/3727620>.
- [14] E. L. LIMA, *The Jordan-Brouwer separation theorem for smooth hypersurfaces*, The American Mathematical Monthly, 95 (1988), pp. 39–42, <http://www.jstor.org/stable/2323445>.
- [15] W. S. MASSEY, *Algebraic Topology: An Introduction*, Springer, New York, 1st ed., 1977.
- [16] S. OSHER AND J. A. SETHIAN, *Fronts propagating with curvature-dependent speed: Algorithms based on Hamilton-Jacobi formulations*, J. Comput. Phys., 79 (1988), pp. 12–49.
- [17] Y. QIU AND Q. ZHANG, *A linear MARS method for three-dimensional interface tracking*, 2025, <https://arxiv.org/abs/2512.07524>.

- [18] A. A. G. REQUICHA, *Mathematical models of rigid solid objects*, Technical Memorandum 28, The University of Rochester, Rochester NY, November 1977.
- [19] A. A. G. REQUICHA AND H. B. VOELCKER, *Solid modeling: current status and research directions*, IEEE Computer Graphics and Applications, 3 (1983), pp. 25–37.
- [20] A. G. REQUICHA AND R. B. TILOVE, *Mathematical foundations of constructive solid geometry: General topology of closed regular sets*, tech. report, University of Rochester, Rochester, N.Y., 1978. <http://hdl.handle.net/1802/1209>.
- [21] J. J. ROTMAN, *An Introduction to Algebraic Topology*, Springer, New York, 1988.
- [22] H. SAGAN, *An elementary proof that Schoenberg’s space-filling curve is nowhere differentiable*, Mathematics Magazine, 65 (1992), pp. 125–128.
- [23] W. SCHMALTZ, *The Jordan-Brouwer separation theorem*, (2009). <https://www.math.uchicago.edu/~may/VIGRE/VIGRE2009/REUPapers/Schmaltz.pdf>.
- [24] S. SEITZ, B. CURLLESS, J. DIEBEL, D. SCHARSTEIN, AND R. SZELISKI, *A comparison and evaluation of multi-view stereo reconstruction algorithms*, in 2006 IEEE Computer Society Conference on Computer Vision and Pattern Recognition (CVPR’06), vol. 1, 2006, pp. 519–528.
- [25] Y. TAN, Y. QIAN, Z. LI, AND Q. ZHANG, *The multiphase cubic MARS method for fourth- and higher-order interface tracking of two or more materials with arbitrarily complex topology and geometry*, 2025, <https://arxiv.org/abs/2506.11897>.
- [26] T. J. TAUTGES, *The common geometry module (CGM): A generic, extensible geometry interface*, in 9th International Meshing Roundtable, New Orleans, LA, USA, 2000, pp. 337–348.
- [27] G. TRYGGVASON, B. BUNNER, D. JURIC, W. TAUBER, S. NAS, J. HAN, N. AL-RAWAHLI, AND Y.-J. JAN, *A front-tracking method for the computations of multiphase flow*, J. Comput. Phys., 169 (2001), pp. 708–759.
- [28] G. TURK AND J. F. O’BRIEN, *Modelling with implicit surfaces that interpolate*, ACM Trans. Graph., 21 (2002), p. 855–873, <https://doi.org/10.1145/571647.571650>.
- [29] J. YANG AND X. JIA, *Overlap region extraction of two NURBS surfaces*, ACM Trans. Graph. (SIGGRAPH Asia), 44 (2025).
- [30] Q. ZHANG, *On donating regions: Lagrangian flux through a fixed curve*, SIAM Review, 55 (2013), pp. 443–461.
- [31] Q. ZHANG, *HFES: a height function method with explicit input and signed output for high-order estimations of curvature and unit vectors of planar curves*, SIAM J. Numer. Anal., 55 (2017), pp. 1024–1056.
- [32] Q. ZHANG, *Fourth- and higher-order interface tracking via mapping and adjusting regular semi-analytic sets represented by cubic splines*, SIAM J. Sci. Comput., 40 (2018), pp. A3755–A3788.
- [33] Q. ZHANG AND A. FOGELSON, *MARS: An analytic framework of interface tracking via mapping and adjusting regular semi-algebraic sets*, SIAM J. Numer. Anal., 54 (2016), pp. 530–560.
- [34] Q. ZHANG AND Z. LI, *Boolean algebra of two-dimensional continua with arbitrarily complex topology*, Math. Comput., 89 (2020), pp. 2333–2364. <https://doi.org/10.1090/mcom/3539>.
- [35] Y. ZHANG, R. ROHLING, AND D. K. PAI, *Direct surface extraction from 3D freehand ultrasound images*, in Proceedings of the Conference on Visualization ’02, 2002, p. 45–52.